Analysis of high-resolution spectra of SiF4 combination bands

M. Merkulova, V. Boudon, L. Manceron

Graphical Abstract

Analysis of high-resolution spectra of SiF_4 combination bands.

M. Merkulova, V. Boudon, L. Manceron

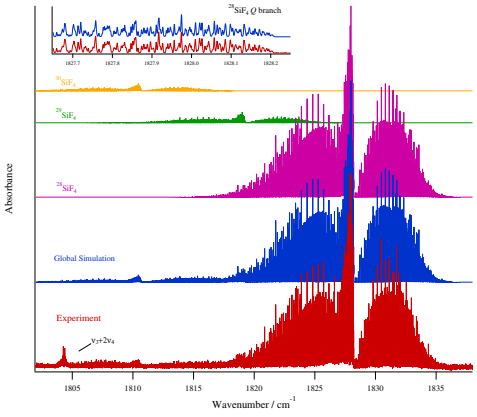

Highlights

Analysis of high-resolution spectra of SiF_4 combination bands.

M. Merkulova, V. Boudon, L. Manceron

- High resolution analysis of $\nu_1+\nu_3$, $\nu_1+\nu_4$, $\nu_2+\nu_3$ and $\nu_2+\nu_4$ combination bands of SiF_4.
- Combination bands of the $^{28}SiF_4$, $^{29}SiF_4$ and $^{30}SiF_4$ isotopologues.
- Determination of spectroscopic parameters.

Analysis of high-resolution spectra of SiF_4 combination bands.

M. Merkulova[b,a], V. Boudon[a,*], L. Manceron[c,d]

[a] *Laboratoire Interdisciplinaire Carnot de Bourgogne, UMR 6303 CNRS - Université Bourgogne Franche-Comté, 9 Av. A. Savary, BP 47870, F-21078 Dijon Cedex, France*
[b] *Research School of High-Energy Physics, National Research Tomsk Polytechnic University, 30 Lenin avenue, 634050 Tomsk, Russia*
[c] *Synchrotron SOLEIL, AILES Beamline, L'Orme des Merisiers, BP48, F-91192 St-Aubin Cedex, France*
[d] *MONARIS, UMR 8233, CNRS-Université, 4 Place Jussieu, case 49, F-75252 Paris Cedex 05, France*

Abstract

The infrared spectra of the silicon tetrafluoride molecule (SiF_4) recorded on the AILES Beamline of the SOLEIL Synchrotron facility, have been studied in the range where the combination bands $\nu_1+\nu_3$, $\nu_1+\nu_4$, $\nu_2+\nu_3$ and $\nu_2+\nu_4$ are located. For each band, between 1100 and more than 2300 lines have been assigned and fitted with the effective Hamiltonian model for J values up to 55 (up to 82 for $\nu_1+\nu_3$). The obtained set of spectroscopic parameters allows one to reproduce experimentally obtained line positions with a root mean square deviation better than $d_{\rm rms} = 0.863 \times 10^{-3}$ cm^{-1}.

Keywords:
High-resolution molecular spectroscopy, SiF_4, Determination of spectroscopic parameters, Spherical top molecule

1. Introduction

Silicon tetrafluoride (SiF_4) is interesting from both practical and theoretical points of view. It is used in electronics and semiconductor industry, as well as for silicon cleaning and etching. Early decomposition of the silicon precursor leads to excessive nucleation of the silicon gas phase and the formation of solid particles, which ultimately affects the quality of the epitaxial growth [1]. This molecule is also formed during volcanic activity [2, 3]. This gas is highly toxic because it releases extremely poisonous hydrogen fluoride (HF) on contact with hot water and acids. Therefore, it is necessary to be able to detect this compound in the atmosphere with high accuracy. The SiF_4 content in volcanic plumes is also a marker of deep magma inside in some volcanoes [4, 5]. Ground-penetrating thermal infrared spectroscopy, which uses radiation from the volcano itself, allows continuous monitoring of the SiF_4 content in the air [4, 5]. It has also been suggested that SiF_4 could be present in Jupiter's volcanic

*Corresponding author
Email address: Vincent.Boudon@u-bourgogne.fr (V. Boudon)

moon Io [6]. Thus, a better knowledge of spectroscopic parameters is needed for this molecule in order to know accurate concentrations.

From a theoretical point of view, the SiF_4 molecule is a spherical top molecule (STM), and, along with other molecules, is a prototype in the study of many more complex molecules. The particular features of STM, which were initially seen as difficulties to be removed, became the motivation that led to original modeling methods applicable to a wide range of spectroscopic problems (see [7] and references therein).

Although they can be used to derive molecular spectroscopic parameters, intramolecular interaction potentials are in general difficult to derive. Given the position of the nuclei and the number of electrons, the *ab initio* quantum chemical calculation methods can be used to solve the electronic Schrödinger equation to compute these potentials, as well as energy, electron densities and other properties of the molecule. In the field of astrochemistry/molecular spectroscopy, in which a lot of molecular species have been observed from the different molecular clouds in the interstellar medium or in planetary atmospheres, *ab initio* quantum chemical calculations also have played a major role both in the laboratory and in observation. It allowed to obtain the necessary spectroscopic parameters for astronomical searches of various molecular species, including molecules with physical conditions that are not easily observable under laboratory conditions [8]. The analysis of high-resolution molecular spectra using effective Hamiltonian, which can be defined as the *semiempirical* method, provides key parameters that can constrain and refine *ab initio* potentials.

Spectroscopic studies of SiF_4 in different spectral ranges can thus provide a more detailed understanding of the molecular structure (bond lengths and angles) and properties, such as the quantum mechanical features, as well as intra and intermolecular dynamical processes. Some of the first theoretical and experimental studies of silicon tetrafluoride were carried out more than half a century ago [9, 10, 11] and, mainly, they did not cover so much of the spectroscopic data of the molecule itself, but rather the computed vibrational frequencies of CX_4-type molecules, force constants and reinvestigated the molecular structure of gaseous SiF_4 [12]. In subsequent studies, [13, 14, 15] authors explored the ν_3 fundamental and $3\nu_3$ band which have been analyzed using both Doppler-limited diode laser spectroscopy and sub-Doppler saturation spectroscopy, both infrared and microwave transitions have been assigned. The next few years of work devoted to the study of this molecule covered some theoretical calculations, Hamiltonian model improvement, double resonance measurement and improvement of ground state using the data on ν_3 band [16, 17]. Also, the second-order Stark effect, splitting the ground state levels of SiF_4 have been observed [18, 19, 20, 21, 22]. Thus, the main attention of researchers for a long time was focused on the study of the ν_3 band and of the ground state, which influenced the further development of theoretical and experimental methods for studying this molecule. Subsequently, the authors of the works [23, 3] presented their results for the calculation of the equilibrium structure, thermodynamic and kinetic parameters of the silicon tetrafluoride molecule. In reference [24] authors have measured integral intensities of absorption bands of gaseous silicon tetrafluoride. With the development of experimental techniques and spherical top theory [25] in some of the recent works [26, 27], a better knowledge of spectroscopic parameters of the fundamentals, overtone and combinations obtained, that led to an accurate determination of the Si-F equilibrium

bond length. A first fit [26, 27] of the dipole moment derivative for the ν_3 band for $^{28}SiF_4$ was performed. With knowledge of the data on fundamental bands, it became possible to study more complex combination bands of the molecule, which are presented in this paper.

The article is organized as follows. Details of experiment are presented in Section 2. Section 3 is dedicated to theoretical background of the study. The analysis on SiF_4 spectra and statistical information of the combination bands study are considered in Section 4, and the results of the spectra analysis are presented in the Section 5.

2. Experiment

The overview spectra is shown in figure 1. Our investigation includes four combination bands, namely $\nu_1+\nu_3$ (near 1528 cm^{-1}), $\nu_1+\nu_4$ (near 1190 cm^{-1}), $\nu_2+\nu_3$ (near 1295 cm^{-1}) and $\nu_2+\nu_4$ (near 653 cm^{-1}). Due to the presence of many hot bands in the spectra of combination bands, a low temperature was required. For most combination bands except $\nu_1+\nu_4$, because of their weak intensity, a long optical path length was also necessary. All spectra were recorded on the AILES Beamline of the SOLEIL Synchrotron facility. The synchrotron light source was coupled to the Bruker 125HR interferometer for the far IR spectra and a glow bar source with variable iris sizes in the mid infrared. The AILES cryogenic short cell or the long path cell, were used with optical path lengths varied from 0.05 to 93 m. Both cells were regulated at 163 K temperature along the entire optical path. The wavenumber scale was calibrated using water, CO_2 or COS trace impurity absorption [28], with a standard deviation of about 3 $\times 10^{-4}$ cm^{-1}. The spectral resolution used for the spectra presented here was varied between 0.002 and 0.004 cm^{-1}. Table 1 summarizes the main experimental conditions; more experimental details can be found in references [26] and [27].

[Table 1 about here.]

[Figure 1 about here.]

3. Theoretical Background

The silicon tetrafluoride is a tetrahedral spherical top molecule with T_d. Due to the high symmetry, the theoretical analysis is based on previous fundamental references such as [29, 30, 31, 32, 33], and on the tensorial formalism and group theory methods developed in the Dijon group [34, 35, 25].

The SiF_4 has four normal modes of vibration: ν_1 (A_1 symmetry 800.7 cm^{-1}), ν_2 (E symmetry 264.2 cm^{-1}), ν_3 and ν_4 (F_2 symmetry, 1031.5 and 388.4 cm^{-1}, respectively). For this molecule type, there exist some simple approximate relations between its vibrational normal mode wavenumbers, leading to groups of vibrational levels called polyads. This approximate relation can also be expressed in vibrational states satisfying the relation

$$k = 6v_1 + 2v_2 + 8v_3 + 3v_4. \quad (1)$$

which thus lead to the usual silane polyads: P_0 (the ground state), P_1 does not exist here, but the level $v_2 = 1$ (0, 1, 0, 0) constitutes polyad P_2, *etc.* Figure 2 schematically presents these polyads (the color markers are as follows: red is for previously analyzed transitions; magenta is for transitions analyzed in the present paper; dashed magenta is for transitions simulated but not fitted yet; blue is for transitions which are still to be analyzed; and dashed blue is for very weak transitions, which are not to be analyzed using the existing spectra).

[Figure 2 about here.]

It should be emphasized that, as a simple calculation of first-order perturbations shows, the contribution of interactions between different vibrational-rotational modes turns out to be surprisingly small in the case of molecules of XF_4 type. Thus, bands can first be analysed with satisfactory accuracy using isolated band models, although, at a later stage, will shall consider a more global analysis by including all data in the above-described polyad scheme. However, the high symmetry of the molecule leads to a complicated additional problem, namely, the presence of tetrahedral splittings in both vibrational and vibrational-rotational states. This, in turn, leads to the necessity to use a rather complicated mathematical apparatus of the theory of irreducible tensor systems to describe the spectrum.

As it is known from the general vibrational-rotational theory [36, 37], the Hamiltonian of an arbitrary polyatomic molecule can be represented as:

$$H^{vib-rot} = \sum_{a,b} |a\rangle\langle b| H^{a,b}, \tag{2}$$

where $|a\rangle$ and $\langle b|$ are vibrational basis functions; $H^{a,b}$ operators depends only on rotational operators $J_\alpha (\alpha = x, y, z)$. In our case, since the molecule has a high symmetry, the equation 2 can be rewritten in a symmetrized form:

$$\begin{aligned} H^{\text{vib}-\text{rot}} &= \sum_{\upsilon\gamma,\upsilon'\gamma'} \sum_{n\Gamma} [(|\upsilon\gamma\rangle \otimes \langle\upsilon'\gamma'|)^{(n\Gamma)} \otimes H^{(n\Gamma)}_{\upsilon\gamma,\upsilon'\gamma'}]^{(A_1)} \\ &\equiv \sum_{\upsilon\gamma,\upsilon'\gamma'} \sum_{n\Gamma} \sum_{\Omega K} [(|\upsilon\gamma\rangle \otimes \langle\upsilon'\gamma'|)^{(n\Gamma)} \otimes R^{\Omega(K,n\Gamma)}]^{(A_1)} Y^{\Omega(K,n\Gamma)}_{\upsilon\gamma,\upsilon'\gamma'}, \end{aligned} \tag{3}$$

where $|\upsilon\gamma\rangle$ is a symmetrized oscillatory function; γ and γ' are the types of function symmetries; $R^{\Omega(K,n\Gamma)}$ is a symmetrized rotational operator, and Ω is the degree of rotation operators $J_\alpha (\alpha = x, y, z)$ for each R operator; K is the rank of this operator; Γ is symmetry in a point symmetry group T_d, and n marks out the different operators $R^{\Omega(K,n\Gamma)}$, having the same meaning Ω, K and Γ. The symbol $\otimes$ denotes the tensoral product, and $Y^{\Omega(K,n\Gamma)}_{\upsilon\gamma,\upsilon'\gamma'}$ values include spectroscopic parameters of different types (for example, the Fermi-type interactions and Coriolis-type interactions). The rotational operators $R^{\Omega(K,n\Gamma)}$, symmetrized in the group T_d, are defined as follows:

$$R^{\Omega(K,n\Gamma)} = \sum_{m}^{(K)} G^m_{n\Gamma\sigma} R^{\Omega(K)}_m, \tag{4}$$

where the operators $R^{\Omega(K)}_m$ are so-called irreducible rotational operators symmetrized with respect to a complete orthogonal group $O(3)$ [38], thanks to the G orientation matrix [39].

The expression of vibrational operators is somewhat "hidden" in the notation of equation 3, inside the $Y^{\Omega(K,n\Gamma)}_{v\gamma,v'\gamma'}$ quantities. This approach from the Tomsk group [40] is, however, strictly equivalent to that of the Dijon Group [34]. The Y contain reduced matrix elements of vibrational operators V, for which we quickly recall hereafter the definition. Due to the existence of the doubly degenerate normal mode $\nu_2(E)$, the systematic generation of vibrational operators requires the use of tensor coupling scheme in the T_d group. For reasons given in references [34], it is helpful to consider creation and annihilation elementary operators expressed in terms of the dimensionless normal coordinates by

$$\begin{array}{ll} a_{s\sigma} = \frac{1}{\sqrt{2}}\,(q_{s\sigma} + ip_{s\sigma}) & (annihilation), \\ a^{+}_{s\sigma} = \frac{1}{\sqrt{2}}\,(q_{s\sigma} - ip_{s\sigma}) & (creation). \end{array} \tag{5}$$

Here, the terms $q_{s\sigma}$ and $ip_{s\sigma}$ are dimensionless operators defined in terms of the normal coordinates $Q_{s\sigma}$. The generic nomenclature for annihilation (or creation) operators is $A^{\Omega(\Gamma)}_s$ (or $A^{+\Omega(\Gamma)}_s$), where s = 1, 2, 3 or 4 denotes the normal mode, Ω is the vibrational degree in elementary operator $a_{s\sigma}$ (or $a^{+}_{s\sigma}$), $\Gamma = A_1$, A_2, E, F_1 or F_2 is the symmetry species relative to the T_d group. Explicit expressions for A and A^+ depend on the degeneracy of the oscillator. We omit the expressions for tensor powers given in [34], however, we note that those expressions follow the same coupling rules and are derived by transforming the expressions for a^+ and a. In all cases $A^{+\Omega(\Gamma)}_s$ is the hermitian conjugate of $A^{\Omega(\Gamma)}_s$.

Vibration operators of symmetry Γ may be formed by coupling creation and annihilation operators in that orders as

$$(A^{+(\gamma_1,\Gamma_1)} \times A^{(\gamma_2,\Gamma_2)})^{(\Gamma)}_{\sigma}. \tag{6}$$

If $\gamma_1 = \gamma_2$ and $\Gamma_1 = \Gamma_2$, hermitian operators are given by

$${}^{\varepsilon}V^{\Gamma_1\Gamma_2(\Gamma)}_{\gamma_1\gamma_2\sigma} = \frac{e^{i\phi}}{N}\,(A^{+(\gamma_1,\Gamma_1)} \times A^{(\gamma_2,\Gamma_2)})^{(\Gamma)}_{\sigma}, \tag{7}$$

where N is a normalizing factor. The parity ε in conjugate momenta $p_{s\sigma}$ and the phase factor $e^{i\phi}$ depends on the parity of the symmetry species Γ. For Γ even ($\Gamma = A_1$, E or F_2), the operator V is necessarily even, and $e^{i\phi}$ has to be real. For Γ odd ($\Gamma = A_2$ or F_1), the operator V is necessarily odd, and $e^{i\phi}$ should be imaginary.

If $\gamma_1 \neq \gamma_2$ or $\Gamma_1 \neq \Gamma_2$, two hermitian combinations may be constructed according to

$${}^{\varepsilon}V^{\Gamma_1\Gamma_2(\Gamma)}_{\gamma_1\gamma_2\sigma} = \frac{e^{i\phi}}{N}\,((A^{+(\gamma_1,\Gamma_1)} \times A^{(\gamma_2,\Gamma_2)})^{(\Gamma)}_{\sigma} + \xi(A^{+(\gamma_2,\Gamma_2)} \times A^{(\gamma_1,\Gamma_1)})^{(\Gamma)}_{\sigma}), \tag{8}$$

where ϕ and ξ depend on the parity ε of the desired operator. Even operators are obtained (whatever the parity of Γ) by setting $\xi = (-1)^{\Gamma_1+\Gamma_2+\Gamma}$ and $e^{i\phi} = 1$. Odd operators are obtained by setting $\xi = -(-1)^{\Gamma_1+\Gamma_2+\Gamma}$ and $e^{i\phi} = -i$. Note that $(-1)^{\Gamma_1+\Gamma_2+\Gamma} = (-1)^{\Gamma_1}(-1)^{\Gamma_2}(-1)^{\Gamma}$ with $(-1)^{\Gamma} = 1$ for $\Gamma = A_1, E$ or F_2 and -1 for $\Gamma = A_2$ or F_1.

Such an ordering of creation-annihilation coupling induces some kind of selection rules resulting from special properties of vibrational matrix elements. The reader wishing to view the discussion of it and the definition of normalising factors, is referred for reference [34], which has a detailed explanation of all mathematical procedures, which, due to their volume, cannot be fully given in this paper.

4. Analysis on SiF_4 spectra in combination bands region

4.1. General considerations

At the initial stage of solving the inverse spectroscopic problem the values of the fundamental band parameters from [27] have been taken as the reference values of the effective Hamiltonian constants. For the transition assignment the software tools SPVIEW has been used [35]. To compute and analyze the energy structure of the (v_1=v_3=1), (v_1=v_4=1), (v_2=v_3=1) and (v_2=v_4=1) vibrational states, the XTDS software package [35] has been used for calculations, fits and simulations. The main difficulty in assigning the spectrum was the presence of lines belonging to the hot bands of the SiF_4 molecule.

Despite the experimental conditions (low temperature), chosen in such a way as to reduce the intensity of the hot bands, some particularly intense lines starting from excited states are still visible in the spectrum (see figure 5, for example), intersecting and sometimes overlapping the lines of the studied bands. However, despite the close location of the centers of hot and cold bands, their interaction, as described above, can be ignored, which still made it possible to solve the inverse spectroscopic problem with high accuracy without taking into account resonant interactions.

4.2. The $\nu_1 + \nu_4$ and $\nu_2 + \nu_3$ bands

For the ν_1+ν_4 (figure 3) and ν_2+ν_3 (figure 4) bands 1130 and 2220 lines have been assigned, respectively. In the ν_1+ν_4 spectra region it was possible to identify the band center for $^{29}SiF_4$ isotopologue, but since these lines are too weak (see details on figure 3), it was not possible to fit any parameters for this isotopoloque band, due to lack of sufficient lines data. On the experimental part of a figure 3 in the centred region we note lines corresponding to the presence of hot bands in this spectrum.

[Table 2 about here.]

[Figure 3 about here.]

The parameter fitting for these bands were made with standard deviation $d_{\mathrm{rms}} = 0.422 \times 10^{-3}$ cm^{-1} for ν_1+ν_4 and $d_{\mathrm{rms}} = 0.336 \times 10^{-3}$ cm^{-1} for ν_2+ν_3, respectively. The calculated band center values are then 1189.9905 cm^{-1}, 1295.4578 cm^{-1} and 1293.9233 cm^{-1} for $\nu_1 + \nu_4(F_2)$, $\nu_2 + \nu_3(F_1)$ and $\nu_2 + \nu_3(F_2)$ sublevels respectively.

[Table 3 about here.]

[Figure 4 about here.]

4.3. The $\nu_2 + \nu_4$ band region

The analysis of the ν_2+ν_4 band was complicated by the presence of a hot ν_3-ν_4 band whose line intensity is similar to the band under study (figure 5). For this band only 722 lines were

assigned, with standard deviation $d_{\mathrm{rms}} = 0.581 \times 10^{-3}$ cm^{-1} (figure 6). The calculated band centers are then 653.0783 cm^{-1} and 653.2995 cm^{-1}, for the F_1 and F_2 sublevels, respectively. For the global simulation we used data on the fundamental bands ν_3 and ν_4 of the molecule [27] to calculate the $\nu_3 - \nu_4$ hot band spectrum.

[Table 4 about here.]

[Figures 5 about here.]

[Figures 6 about here.]

4.4. The $\nu_1 + \nu_3$ band

For the ν_1+ν_3 band it was possible to fit also the parameters, corresponding to the $^{29}SiF_4$ and $^{30}SiF_4$ isotopologues with about 1330, 198 and 267 lines for each isotopic modification, respectively. As the reader can see on figure 7, the global simulation for all the isotopologues shows a good agreement with the experiment. The parameters have been fitted for $^{28}SiF_4$, $^{29}SiF_4$ and $^{30}SiF_4$ with the standard deviation as follows: $^{28}d_{\mathrm{rms}} = 0.863 \times 10^{-3}$ cm^{-1}, $^{29}d_{\mathrm{rms}} = 0.765 \times 10^{-3}$ cm^{-1} and $^{30}d_{\mathrm{rms}} = 0.480 \times 10^{-3}$ cm^{-1}.

[Figure 7 about here.]

[Table 5 about here.]

The calculated band center values are then 1828.3546 cm^{-1}, 1819.3854 cm^{-1} and 1810.8235 cm^{-1} for $^{28}SiF_4$, $^{29}SiF_4$ and $^{30}SiF_4$, respectively.

4.5. Fit residuals and line lists

The final fit residuals for each band are shown on figure 8, the list of the fitted parameters for each band are shown in the Tables 1-4.

Line lists of assigned lines for the four different bands studied in this paper are provided as Supplementary Material.

[Figure 8 about here.]

5. Conclusion

The spectrum of the silicon tetrafluoride molecule SiF_4 was explored in four combination band ranges. Using the tools for the analysis and simulation, described in reference [35], we determined the energy structure of the ($v_1 = v_3$=1), ($v_1 = v_4$=1), ($v_2 = v_3$=1) and ($v_2 = v_4$=1) vibrational stage. More than 5870 transitions were assigned with the J_{max} values up to 55 (up to 82 for ν_1+ν_3) and this leads to a determination of accurate molecular

parameters with root mean square deviations for line positions of a few 10^{-4} cm^{-1}. In the case of the ν_1+ν_3 band, the $^{29}SiF_4$ and $^{30}SiF_4$ isotopologues could also be assigned and fitted (figure 3). These results will allow the calculation of hot bands like ν_3+ν_2-ν_2, *etc.*, in the regions of strong atmospheric absorption. The results obtained are also important for their further use in the high-precision semi-empirical determination of the intramolecular potential function of tetrafluorosilane, as well as for the subsequent analysis of the line intensities of this molecule.

Acknowledgments

MM thanks ISITE-UBFC for supporting her PhD during her stay in France. We also grateful to the Synchrotron SOLEIL (Project 20200349), France for supporting this work.

References

[1] T. Rana, M. Chandrashekhar, K. Daniels, T. Sudarshan, SiC Homoepitaxy, Etching and Graphene Epitaxial Growth on SiC Substrates Using a Novel Fluorinated Si Precursor Gas (SiF_4), Journal of Electronic Materials 45 (2016) 2019–2024.

[2] N. Taquet, I. Meza Hernández, W. Stremme, A. Bezanilla, M. Grutter, R. Campion, M. Palm, T. Boulesteix, Continous measurements of SiF_4 and SO_2 by thermal emission spectroscopy: Insight from a 6-month survey at the Popocatépelt volcano, J. Volcanol. Geotherm. Res. 341 (2017) 255–268.

[3] S. K. Ignatov, P. G. Sennikov, L. A. Chuprov, A. G. Razuvaev, Thermodynamic and kinetic parameters of elementary steps in gas-phase hydrolysis of SiF_4. Quantum−chemical and FTIR spectroscopic studies, Russian chemical bulletin 52 (2003) 837–845.

[4] W. Stremme, A. Krueger, R. Harig, M. Grutter, Volcanic SO_2 and SiF_4 visualization using 2-D thermal emission spectroscopy – Part 1: Slant-columns and their ratios, Atmos. Meas. Tech. 5 (2012) 275–288.

[5] A. Krueger, W. Stremme, R. Harig, M. Grutter, Volcanic SO_2 and SiF_4 visualization using 2-D thermal emission spectroscopy – Part 2: Wind propagation and emission rates, Atmos. Meas. Tech. 6 (2013) 47–61.

[6] L. Schaefer, B. Fegley Jr., Silicon tetrafluoride on Io, Icarus 179 (2005) 252–258.

[7] V. Boudon, J.-P. Champion, T. Gabard, M. Loëte, M. Rotger, C. Wenger, Spherical top theory and molecular spectra, in: M. Quack, F. Merkt (Eds.), Handbook of High-Resolution Spectroscopy, Vol. 3, Wiley, Chichester, West Sussex, United Kingdom, 2011, pp. 1437–1460.

[8] E. E. Etim, S. A. Olagboye, O. E. Godwin, I. M. Atiatah, Quantum chemical studies on silicon tetrafluoride and its protonated analogues, International Journal of Modern Chemistry and Applied Science 12 (1) (2020) 26–45.

[9] T. Shimanouchi, I. Nakagawa, J. Hiraishi, M. Ishii, Force constants of CF_4, SiF_4, BF_3, CH_4, SiH_4, NH_3 and PH_3, J. Mol. Spectrosc. 19 (1966) 78–107.

[10] R. Clark, D. Rippon, The vapor-phase Raman spectra, Raman band contour analyses, Coriolis constants, and force constants of spherical-top molecules MX_4 (M = Group IV element, X = F, Cl, Br or I), J. Mol. Spectrosc. 44 (1972) 479–503.

[11] F. Königer, A. Müller, W. Orville-Thomas, The use of isotopic substitution and matrix isolation techniques in determining molecular constants of group IV tetrahalides, J. Mol. Struct. 37 (1977) 199–227.

[12] K. R. Hagen, K. Hedberg, Interatomic distances and rms amplitudes of vibration of gaseous SiF_4 from electron diffraction, The Journal of Chemical Physics 59 (1973) 1549–1550.

[13] C. W. Patterson, R. S. McDowell, N. G. Nereson, B. J. Krohn, J. S. Wells, F. R. Petersen, Tunable laser diode study of the ν_3 band of SiF_4 near 9.7 μm, J. Mol. Spectrosc. 91 (1982) 416–423.

[14] C. W. Patterson, A. S. Pine, Doppler-limited spectrum and analysis of the $3\nu_3$ manifold of SiF_4, J. Mol. Spectrosc. 96 (1982) 404–421.

[15] M. Takami, H. Kuze, Infrared-microwave double resonance spectroscopy of the SiF_4 ν_3 fundamental using a tunable diode laser, J. Chem. Phys. 78 (1983) 2204–2209.
[16] L. Halonen, Stretching vibrational overtone and combination states in silicon tetrafluoride, J. Mol. Spectrosc. 120 (1986) 175–184.
[17] L. Jörissen, W. A. Kreiner, Y.-T. Chen, T. Oka, Observation of ground state rotational transitions in silicon tetrafluoride, J. Mol. Spectrosc. 120 (1986) 233–235.
[18] L. Jörissen, H. Prinz, W. A. Kreiner, Second-order Stark effect observation in the ground state of silicon tetrafluoride, SiF_4, J. Mol. Spectrosc. 124 (1987) 236–239.
[19] L. Jörissen, H. Prinz, W. A. Kreiner, C. Wenger, G. Pierre, G. Magerl, W. Schupita, The ν_3 fundamental of silicon tetrafluoride. Spectroscopy with laser sidebands, Can. J. Phys. 67 (1989) 532–542.
[20] A. Behrendt, L. Jörissen, W. A. Kreiner, M. Loëte, Double-modulation sideband spectroscopy: μ_0 and μ_{33} of silicon tetrafluoride, J. Mol. Spectrosc. 155 (1992) 326–323.
[21] A. Ainetschian, W. A. Kreiner, M.-P. Coquard, M. Loëte, Sideband double modulation: The ground state dipole moment of SiF_4, J. Mol. Spectrosc. 161 (1993) 264–268.
[22] M.-P. Coquard, M. Loëte, A. Ainetschian, W. Kreiner, Prediction and observation of the nonlinear Stark effect in the ν_3 band of SiF_4, J. Mol. Spectrosc. 170 (1995) 251–265.
[23] J. Breidung, J. Demaison, L. Margulés, W. Thiel, Equilibrium structure of SiF_4, Chemical physics letters 313 (1999) 713–717.
[24] A. P. Burtsev, V. N. Bocharov, S. K. Ignatov, T. D. Kolomiĭtsova, P. G. Sennikov, K. G. Tokhadze, L. A. Chuprov, D. N. Shchepkin, O. Schrems, Integral intensities of absorption bands of silicon tetrafluoride in the gas phase and cryogenic solutions: Experiment and Calculation, Optics Spectrosc. 98 (2005) 227–234.
[25] V. Boudon, J.-P. Champion, T. Gabard, M. Loëte, M. Rotger, C. Wenger, Spherical top theory and molecular spectra, in: M. Quack, F. Merkt (Eds.), Handbook of High Resolution Spectroscopy, Vol. 3, John Wiley & Sons, Ltd, Chichester, 2011, Ch. 39, pp. 1437–1460.
[26] V. Boudon, L. Manceron, C. Richard, High-resolution spectroscopy and analysis of the ν_3, ν_4 and $2\nu_4$ bands of SiF_4 in natural isotopic abundance, Journal of Quantitative Spectroscopy and Radiative Transfer 253 (2020) 107114.
[27] V. Boudon, C. Richard, L. Manceron, High-resolution spectroscopy and analysis of the fundamental modes of $^{28}SiF_4$. Accurate experimental determination of the Si-F bond length, Journal of Molecular Spectroscopy 383 (2022) 111549.
[28] L. S. Rothman, I. E. Gordon, A. Barbe, D. C. Benner, P. E. Bernath, M. Birk, V. Boudon, L. R. Brown, A. Campargue, J. P. Champion, K. Chance, L. H. Coudert, V. Dana, V. M. Devi, S. Fally, J. M. Flaud, R. R. Gamache, A. Goldman, D. Jacquemart, I. Kleiner, N. Lacome, W. J. Lafferty, J. Y. Mandin, S. T. Massie, S. N. Mikhailenko, C. E. Miller, N. Moazzen-Ahmadi, O. V. Naumenko, A. V. Nikitin, J. Orphal, V. I. Perevalov, A. Perrin, A. Predoi-Cross, C. P. Rinsland, M. Rotger, M. Simeckova, M. A. H. Smith, K. Sung, S. A. Tashkun, J. Tennyson, R. A. Toth, A. C. Vandaele, J. Vander Auwera, The HITRAN 2008 molecular spectroscopic database, J. Quant. Spectrosc. Radiat. Transfer 110 (2009) 533–572.
[29] H. A. Jahn, A new Coriolis perturbation in the methane spectrum. I. Vibrational-rotational Hamiltonian and wave functions, Proc. Roy. Soc. A 168 (1938) 469–495.
[30] H. A. Jahn, A new Coriolis perturbation in the methane spectrum. II. Energy levels, Proc. Roy. Soc. A 168 (1938) 495–518.
[31] J. Herranz, The rotational structure of the fundamental infrared bands of methane-type molecules, Journal of Molecular Spectroscopy 6 (1961) 343–359.
[32] A. Robiette, D. Gray, F. Birss, The effective vibration-rotation hamiltonian for triply-degenerate fundamentals of tetrahedral XY_4 molecules, Mol. Phys. 32 (1976) 1591–1607.
[33] A. J. Stone, Transformation between cartesian and spherical tensors, Mol. Phys. 29 (1975) 1461–1471.
[34] J.-P. Champion, M. Loëte, G. Pierre, Spherical top spectra, in: K. N. Rao, A. Weber (Eds.), Spectroscopy of the Earth's atmosphere and interstellar medium, Academic Press, San Diego, 1992, pp. 339–422.

[35] C. Wenger, V. Boudon, M. Rotger, J. P. Sanzharov, J. P. Champion, XTDS and SPVIEW: Graphical tools for the analysis and simulation of high-resolution molecular spectra, Journal of Molecular Spectroscopy 251 (2008) 102–113.
[36] D. Papoušek, M. Aliev, Molecular vibrational-rotational spectra, Elsevier, New York, 1982.
[37] O. Ulenikov, G. Onopenko, N. Tyabaeva, S. Alanko, M. Koivusaari, R. Anttila, Precise Study of the Lowest Vibration-Rotational Bands ν_5 and ν_3/ν_6 of the CHD_3 Molecule, Journal of Molecular Spectroscopy 186 (1997) 293–313.
[38] V. Boudon, C. Richard, M. L. B. Willis, Analytical expression of tensorial rotational operators for semi-classical interpretation of molecular spectra. Relations between molecular Hamiltonian parameters in different formalisms, J. Mol. Spectrosc. 385 (2022) 111602.
[39] M. Rey, V. Boudon, C. Wenger, G. Pierre, B. Sartakov, Orientation of $O(3)$ and $SU(2) \otimes C_I$ representations in cubic point groups (O_h, T_d) for application to molecular spectroscopy, J. Mol. Spectrosc. 219 (2003) 313–325.
[40] O. N. Ulenikov, On the determination of spectroscopic constants as functions of intramolecular parameters., J. Phys. B: At. Mol. Opt. Phys. 22 (1989) 997–1015.

Table 1: Experimental conditions for recording the various SiF_4 bands studied in the present work.

Band (source-iris)	Pressure / mb × Path length / m	Temp (K)	# Averaged scans	Resolution / cm^{-1}	Beamsplitter/Detector/cold Filter
ν_2 (Synchrotron)	2.13 × 93	163	252	0.001	Si-My6μm/Bolometer/0–700 cm^{-1}
$\nu_1 - \nu_4$ (Synchrotron).	0.44 × 93	163	360	0.001	Si-My6μm/Bolometer/0–700 cm^{-1}
$\nu_2 + \nu_4$ (Synchrotron)	14.9 × 93	163	604	0.002	Ge-KBr/HgCdTe-4K/400–920 cm^{-1}
$2\nu_4$ (Globar + iris 1.7 mm)	6.35 × 3	163	1680	0.004	Ge-KBr/HgCdTe-4K/400–920 cm^{-1}
$\nu_1 + \nu_4$ (Globar + iris 1.15 mm)	8.6 × 0.051	163	90	0.0015	Ge-KBr/HgCdTe-4K/1100–1900 cm^{-1}
$\nu_2 + \nu_3$ (Globar + iris 1.7 mm)	2.0 × 3	163	1920	0.004	Ge-KBr/HgCdTe-4K/1100–1900 cm^{-1}
$\nu_1 + \nu_3$ (Globar + iris 1.5 mm)	0.49 × 3	163	988	0.002	Ge-KBr/HgCdTe-4K/1100–1900 cm^{-1}

Table 2: Effective Hamiltonian parameters* for the $\nu_1 + \nu_4$ band of $^{28}SiF_4$.

Level	$\Omega(K,nC)$	Γ_ν	Γ'_ν	Value / cm^{-1}	
GS	2(0,0A_1)	0000A_1	0000A_1	1.3778054572	$\times 10^{-1}$
	4(0,0A_1)	0000A_1	0000A_1	-4.1380253094	$\times 10^{-8}$
	4(4,0A_1)	0000A_1	0000A_1	-3.3605104766	$\times 10^{-9}$
	6(0,0A_1)	0000A_1	0000A_1	-2.1026176312	$\times 10^{-14}$
	6(4,0A_1)	0000A_1	0000A_1	2.1485549711	$\times 10^{-15}$
	6(6,0A_1)	0000A_1	0000A_1	3.5386683028	$\times 10^{-16}$
	8(0,0A_1)	0000A_1	0000A_1	1.0153837427	$\times 10^{-17}$
	8(4,0A_1)	0000A_1	0000A_1	1.1571819224	$\times 10^{-19}$
	8(6,0A_1)	0000A_1	0000A_1	3.6235946947	$\times 10^{-20}$
	8(8,0A_1)	0000A_1	0000A_1	-5.4404352192	$\times 10^{-20}$
ν_4	0(0,0A_1)	0001F_2	0001F_2	3.8843327560	$\times 10^{2}$
	1(1,0F_1)	0001F_2	0001F_2	-2.7571733237	$\times 10^{-2}$
	2(0,0A_1)	0001F_2	0001F_2	1.6854597514	$\times 10^{-4}$
	2(2,0E)	0001F_2	0001F_2	-1.1747337405	$\times 10^{-4}$
	2(2,0F_2)	0001F_2	0001F_2	5.5406961794	$\times 10^{-5}$
	3(1,0F_1)	0001F_2	0001F_2	-1.1535825948	$\times 10^{-7}$
	3(3,0F_1)	0001F_2	0001F_2	-2.0262702248	$\times 10^{-7}$
	4(0,0A_1)	0001F_2	0001F_2	-2.6387612421	$\times 10^{-10}$
	4(2,0E)	0001F_2	0001F_2	-1.8420507054	$\times 10^{-10}$
	4(2,0F_2)	0001F_2	0001F_2	7.8780009368	$\times 10^{-11}$
	4(4,0A_1)	0001F_2	0001F_2	-1.2917641567	$\times 10^{-11}$
	4(4,0E)	0001F_2	0001F_2	8.2141441890	$\times 10^{-11}$
	4(4,0F_2)	0001F_2	0001F_2	1.8971322209	$\times 10^{-11}$
ν_1	0(0,0A_1)	1000A_1	1000A_1	8.0066566202	$\times 10^{2}$
	2(0,0A_1)	1000A_1	1000A_1	-1.5877745744	$\times 10^{-4}$
	4(0,0A_1)	1000A_1	1000A_1	6.7084194225	$\times 10^{-10}$
	4(4,0A_1)	1000A_1	1000A_1	4.6999614771	$\times 10^{-11}$
$\nu_1 + \nu_4$	0(0,0A_1)	1001F_2	1001F_2	8.91586(57)	$\times 10^{-1}$
	1(1,0F_1)	1001F_2	1001F_2	2.3974(51)	$\times 10^{-3}$
	2(0,0A_1)	1001F_2	1001F_2	1.628(18)	$\times 10^{-5}$
	2(2,0E)	1001F_2	1001F_2	-1.109(33)	$\times 10^{-5}$
	2(2,0F_2)	1001F_2	1001F_2	2.21(44)	$\times 10^{-6}$
	3(1,0F_1)	1001F_2	1001F_2	1.05(15)	$\times 10^{-8}$
	d_{rms}	0.417	$\times 10^{-3}$		
	J_{max}	58			

* Values with no uncertainty are fixed to the fundamental band parameters [27].

Table 3: Effective Hamiltonian parameters* for the $\nu_2 + \nu_3$ band of $^{28}SiF_4$.

Level	$\Omega(K,nC)$	Γ_ν	Γ'_ν	Value / cm^{-1}		Level	$\Omega(K,nC)$	Γ_ν	Γ'_ν	Value / cm^{-1}	
GS	2(0,0A$_1$)	0000A$_1$	0000A$_1$	1.3778054572	$\times10^{-1}$		5(3,0F$_1$)	0010F$_2$	0010F$_2$	-1.9792627703	$\times10^{-12}$
	4(0,0A$_1$)	0000A$_1$	0000A$_1$	-4.1380253094	$\times10^{-8}$		5(5,0F$_1$)	0010F$_2$	0010F$_2$	4.7126915343	$\times10^{-12}$
	4(4,0A$_1$)	0000A$_1$	0000A$_1$	-3.3605104766	$\times10^{-9}$		5(5,1F$_1$)	0010F$_2$	0010F$_2$	-9.1292709636	$\times10^{-12}$
	6(0,0A$_1$)	0000A$_1$	0000A$_1$	-2.1026176312	$\times10^{-14}$		6(2,0E)	0010F$_2$	0010F$_2$	-1.4624471868	$\times10^{-13}$
	6(4,0A$_1$)	0000A$_1$	0000A$_1$	2.1485549711	$\times10^{-15}$		6(2,0F$_2$)	0010F$_2$	0010F$_2$	1.4374793642	$\times10^{-13}$
	6(6,0A$_1$)	0000A$_1$	0000A$_1$	3.5386683028	$\times10^{-16}$		6(4,0A$_1$)	0010F$_2$	0010F$_2$	-8.2612218488	$\times10^{-15}$
	8(0,0A$_1$)	0000A$_1$	0000A$_1$	1.0153837427	$\times10^{-17}$		6(4,0E)	0010F$_2$	0010F$_2$	2.3983009358	$\times10^{-13}$
	8(4,0A$_1$)	0000A$_1$	0000A$_1$	1.1571819224	$\times10^{-19}$		6(4,0F$_2$)	0010F$_2$	0010F$_2$	1.7444078013	$\times10^{-13}$
	8(6,0A$_1$)	0000A$_1$	0000A$_1$	3.6235946947	$\times10^{-20}$	ν_2+ν_3	0(0,0A$_1$)	0110F$_1$	0110F$_1$	-3.0613(15)	$\times10^{-1}$
	8(8,0A$_1$)	0000A$_1$	0000A$_1$	-5.4404352192	$\times10^{-20}$		1(1,0F$_1$)	0110F$_1$	0110F$_1$	2.084(12)	$\times10^{-3}$
ν_2	0(0,0A$_1$)	0100E	0100E	2.6421952537	$\times10^{2}$		2(0,0A$_1$)	0110F$_1$	0110F$_1$	-8.52(24)	$\times10^{-6}$
	2(0,0A$_1$)	0100E	0100E	-1.4308354627	$\times10^{-4}$		2(2,0F$_2$)	0110F$_1$	0110F$_1$	9.06(34)	$\times10^{-6}$
	2(2,0E)	0100E	0100E	-4.6789319673	$\times10^{-5}$		3(1,0F$_1$)	0110F$_1$	0110F$_1$	2.69(77)	$\times10^{-8}$
	3(3,0A$_2$)	0100E	0100E	1.4181259250	$\times10^{-7}$		3(3,0F$_1$)	0110F$_1$	0110F$_1$	-2.772(98)	$\times10^{-7}$
	4(0,0A$_1$)	0100E	0100E	3.9106906991	$\times10^{-10}$		4(2,0E)	0110F$_1$	0110F$_1$	-1.014(37)	$\times10^{-9}$
	4(2,0E)	0100E	0100E	-1.0089916064	$\times10^{-10}$		4(2,0F$_2$)	0110F$_1$	0110F$_1$	2.89(55)	$\times10^{-10}$
	4(4,0A$_1$)	0100E	0100E	3.5353220309	$\times10^{-11}$		1(1,0F$_1$)	0110F$_1$	0110F$_2$	2.480(67)	$\times10^{-4}$
	4(4,0E)	0100E	0100E	-7.7457552175	$\times10^{-11}$		2(2,0F$_2$)	0110F$_1$	0110F$_2$	6.488(55)	$\times10^{-6}$
	5(3,0A$_2$)	0100E	0100E	3.2257385749	$\times10^{-13}$		3(1,0F$_1$)	0110F$_1$	0110F$_2$	-7.55(44)	$\times10^{-8}$
ν_3	0(0,0A$_1$)	0010F$_2$	0010F$_2$	1.0315444382	$\times10^{3}$		3(3,0A$_2$)	0110F$_1$	0110F$_2$	8.61(47)	$\times10^{-9}$
	1(1,0F$_1$)	0010F$_2$	0010F$_2$	3.1312442955	$\times10^{-1}$		3(3,0F$_1$)	0110F$_1$	0110F$_2$	9.52(53)	$\times10^{-8}$
	2(0,0A$_1$)	0010F$_2$	0010F$_2$	-2.9725440181	$\times10^{-4}$		4(2,0E)	0110F$_1$	0110F$_2$	-2.01(21)	$\times10^{-10}$
	2(2,0E)	0010F$_2$	0010F$_2$	2.5318159947	$\times10^{-4}$		0(0,0A$_1$)	0110F$_2$	0110F$_2$	-1.840624(97)	
	2(2,0F$_2$)	0010F$_2$	0010F$_2$	-0.9960481504	$\times10^{-4}$		1(1,0F$_1$)	0110F$_2$	0110F$_2$	6.1196(90)	$\times10^{-3}$
	3(1,0F$_1$)	0010F$_2$	0010F$_2$	1.0539876659	$\times10^{-7}$		2(0,0A$_1$)	0110F$_2$	0110F$_2$	5.43(22)	$\times10^{-6}$
	3(3,0F$_1$)	0010F$_2$	0010F$_2$	-2.4636618391	$\times10^{-8}$		2(2,0F$_2$)	0110F$_2$	0110F$_2$	-1.883(34)	$\times10^{-5}$
	4(0,0A$_1$)	0010F$_2$	0010F$_2$	9.4179695416	$\times10^{-12}$		3(1,0F$_1$)	0110F$_2$	0110F$_2$	2.201(75)	$\times10^{-7}$
	4(2,0E)	0010F$_2$	0010F$_2$	-5.7413330160	$\times10^{-9}$		3(3,0F$_1$)	0110F$_2$	0110F$_2$	-1.006(97)	$\times10^{-7}$
	4(2,0F$_2$)	0010F$_2$	0010F$_2$	6.2589553124	$\times10^{-9}$		4(2,0E)	0110F$_2$	0110F$_2$	-3.29(32)	$\times10^{-10}$
	4(4,0A$_1$)	0010F$_2$	0010F$_2$	8.7058384570	$\times10^{-11}$		4(2,0F$_2$)	0110F$_2$	0110F$_2$	-2.35(48)	$\times10^{-10}$
	4(4,0E)	0010F$_2$	0010F$_2$	9.2015768930	$\times10^{-9}$		d_{rms}	0.336	$\times10^{-3}$		
	4(4,0F$_2$)	0010F$_2$	0010F$_2$	6.7123543060	$\times10^{-9}$		J_{max}	70			
	5(1,0F$_1$)	0010F$_2$	0010F$_2$	-9.8901362804	$\times10^{-12}$						

* Values with no uncertainty are fixed to the fundamental band parameters [27].

Table 4: Effective Hamiltonian parameters* for the ν_2 + ν_4 band of $^{28}SiF_4$.

Level	$\Omega(K,nC)$	Γ_ν	Γ'_ν	Value / cm^{-1}		Level	$\Omega(K,nC)$	Γ_ν	Γ'_ν	Value / cm^{-1}	
GS	2(0,0A$_1$)	0000A$_1$	0000A$_1$	1.3778054572	$\times10^{-1}$		4(4,0E)	0001F$_2$	0001F$_2$	8.2141441890	$\times10^{-11}$
	4(0,0A$_1$)	0000A$_1$	0000A$_1$	-4.1380253094	$\times10^{-8}$		4(4,0F$_2$)	0001F$_2$	0001F$_2$	1.8971322209	$\times10^{-11}$
	4(4,0A$_1$)	0000A$_1$	0000A$_1$	-3.3605104766	$\times10^{-9}$	ν_2+ν_4	0(0,0A$_1$)	0101F$_1$	0101F$_1$	4.2553(33)	$\times10^{-1}$
	6(0,0A$_1$)	0000A$_1$	0000A$_1$	-2.1026176312	$\times10^{-14}$		1(1,0F$_1$)	0101F$_1$	0101F$_1$	7.00(26)	$\times10^{-4}$
	6(4,0A$_1$)	0000A$_1$	0000A$_1$	2.1485549711	$\times10^{-15}$		2(0,0A$_1$)	0101F$_1$	0101F$_1$	1.879(99)	$\times10^{-5}$
	6(6,0A$_1$)	0000A$_1$	0000A$_1$	3.5386683028	$\times10^{-16}$		2(2,0E)	0101F$_1$	0101F$_1$	-2.68(92)	$\times10^{-6}$
	8(0,0A$_1$)	0000A$_1$	0000A$_1$	1.0153837427	$\times10^{-17}$		2(2,0F$_2$)	0101F$_1$	0101F$_1$	-8.9(1.0)	$\times10^{-6}$
	8(4,0A$_1$)	0000A$_1$	0000A$_1$	1.1571819224	$\times10^{-19}$		3(1,0F$_1$)	0101F$_1$	0101F$_1$	8.83(85)	$\times10^{-8}$
	8(6,0A$_1$)	0000A$_1$	0000A$_1$	3.6235946947	$\times10^{-20}$		4(0,0A$_1$)	0101F$_1$	0101F$_1$	-1.169(23)	$\times10^{-8}$
	8(8,0A$_1$)	0000A$_1$	0000A$_1$	-5.4404352192	$\times10^{-20}$		4(2,0E)	0101F$_1$	0101F$_1$	-5.47(21)	$\times10^{-9}$
ν_2	0(0,0A$_1$)	0100E	0100E	2.6421952537	$\times10^{2}$		4(4,0E)	0101F$_1$	0101F$_1$	-1.59(15)	$\times10^{-9}$
	2(0,0A$_1$)	0100E	0100E	-1.4308354627	$\times10^{-4}$		4(4,0F$_2$)	0101F$_1$	0101F$_1$	4.50(22)	$\times10^{-9}$
	2(2,0E)	0100E	0100E	-4.6789319673	$\times10^{-5}$		1(1,0F$_1$)	0101F$_1$	0101F$_2$	-6.55(26)	$\times10^{-4}$
	3(3,0A$_2$)	0100E	0100E	1.4181259250	$\times10^{-7}$		2(2,0E)	0101F$_1$	0101F$_2$	-1.565(63)	$\times10^{-5}$
	4(0,0A$_1$)	0100E	0100E	3.9106906991	$\times10^{-10}$		3(1,0F$_1$)	0101F$_1$	0101F$_2$	-2.672(53)	$\times10^{-7}$
	4(2,0E)	0100E	0100E	-1.0089916064	$\times10^{-10}$		4(2,0E)	0101F$_1$	0101F$_2$	-2.82(12)	$\times10^{-9}$
	4(4,0A$_1$)	0100E	0100E	3.5353220309	$\times10^{-11}$		4(4,0E)	0101F$_1$	0101F$_2$	2.67(12)	$\times10^{-9}$
	4(4,0E)	0100E	0100E	-7.7457552175	$\times10^{-11}$		4(4,0F$_2$)	0101F$_1$	0101F$_2$	-2.53(60)	$\times10^{-10}$
	5(3,0A$_2$)	0100E	0100E	3.2257385749	$\times10^{-13}$		0(0,0A$_1$)	0101F$_2$	0101F$_2$	6.4666(16)	$\times10^{-1}$
ν_4	0(0,0A$_1$)	0001F$_2$	0001F$_2$	3.8843327560	$\times10^{2}$		1(1,0F$_1$)	0101F$_2$	0101F$_2$	-1.191(14)	$\times10^{-3}$
	1(1,0F$_1$)	0001F$_2$	0001F$_2$	-2.7571733237	$\times10^{-2}$		2(0,0A$_1$)	0101F$_2$	0101F$_2$	-1.784(72)	$\times10^{-5}$
	2(0,0A$_1$)	0001F$_2$	0001F$_2$	1.6854597514	$\times10^{-4}$		2(2,0E)	0101F$_2$	0101F$_2$	-1.425(82)	$\times10^{-4}$
	2(2,0E)	0001F$_2$	0001F$_2$	-1.1747337405	$\times10^{-4}$		2(2,0F$_2$)	0101F$_2$	0101F$_2$	6.12(72)	$\times10^{-6}$
	2(2,0F$_2$)	0001F$_2$	0001F$_2$	5.5406961794	$\times10^{-5}$		3(1,0F$_1$)	0101F$_2$	0101F$_2$	1.369(56)	$\times10^{-7}$
	3(1,0F$_1$)	0001F$_2$	0001F$_2$	-1.1535825948	$\times10^{-7}$		4(2,0E)	0101F$_2$	0101F$_2$	-2.43(17)	$\times10^{-9}$
	3(3,0F$_1$)	0001F$_2$	0001F$_2$	-2.0262702248	$\times10^{-7}$		4(4,0E)	0101F$_2$	0101F$_2$	2.75(16)	$\times10^{-9}$
	4(0,0A$_1$)	0001F$_2$	0001F$_2$	-2.6387612421	$\times10^{-10}$		4(4,0F$_2$)	0101F$_2$	0101F$_2$	-3.2(1.4)	$\times10^{-10}$
	4(2,0E)	0001F$_2$	0001F$_2$	-1.8420507054	$\times10^{-10}$		d_{rms}	0.581	$\times10^{-3}$		
	4(2,0F$_2$)	0001F$_2$	0001F$_2$	7.8780009368	$\times10^{-11}$		J_{max}	55			
	4(4,0A$_1$)	0001F$_2$	0001F$_2$	-1.2917641567	$\times10^{-11}$						

* Values with no uncertainty are fixed to the fundamental band parameters [27].

Table 5: Effective Hamiltonian parameters* for the $\nu_1 + \nu_3$ band of $^{28}SiF_4$, $^{29}SiF_4$ and $^{30}SiF_4$ isotopologues.

Level	$\Omega(K,nC)$	$^{28}SiF_4$ / cm^{-1}	$^{29}SiF_4$ / cm^{-1}	$^{30}SiF_4$ / cm^{-1}	
GS	2(0,0A$_1$)	1.3778054572			$\times10^{-1}$
	2(0,0A$_1$)	1.3778054572			$\times10^{-1}$
	4(0,0A$_1$)	-4.1380253094			$\times10^{-8}$
	4(4,0A$_1$)	-3.3605104766			$\times10^{-9}$
	6(0,0A$_1$)	-2.1026176312			$\times10^{-14}$
	6(4,0A$_1$)	2.1485549711			$\times10^{-15}$
	6(6,0A$_1$)	3.5386683028			$\times10^{-16}$
	8(0,0A$_1$)	1.0153837427			$\times10^{-17}$
	8(4,0A$_1$)	1.1571819224			$\times10^{-19}$
	8(6,0A$_1$)	3.6235946947			$\times10^{-20}$
	8(8,0A$_1$)	-5.4404352192			$\times10^{-20}$
ν_1	0(0,0A$_1$)	8.0066566202			$\times10^{2}$
	2(0,0A$_1$)	-1.5877745744			$\times10^{-4}$
	4(0,0A$_1$)	6.7084194225			$\times10^{-10}$
	4(4,0A$_1$)	4.6999614771			$\times10^{-11}$
ν_3	0(0,0A$_1$)	1.0315444382	1.0225751938	1.0141645348	$\times10^{3}$
	1(1,0F$_1$)	3.1312442955	3.0742156603	3.0173644241	$\times10^{-1}$
	2(0,0A$_1$)	-2.9725440181	-2.9208225910	-2.8760964593	$\times10^{-4}$
	2(2,0E)	2.5318159947	2.4735629711	2.4274475400	$\times10^{-4}$
	2(2,0F$_2$)	-0.9960481504	-0.9655764165	-0.9396328517	$\times10^{-4}$
	3(1,0F$_1$)	1.0539876659	1.0371937471	0.8583725548	$\times10^{-7}$
	3(3,0F$_1$)	-2.4636618391	-4.1655091861	-3.8223718581	$\times10^{-8}$
	4(0,0A$_1$)	9.4179695416			$\times10^{-12}$
	4(2,0E)	-5.7413330160	-5.7383030353	-4.7898162610	$\times10^{-9}$
	4(2,0F$_2$)	6.2589553124	6.3102541995	5.6846430252	$\times10^{-9}$
	4(4,0A$_1$)	8.7058384570	8.6875322090	8.6875322090	$\times10^{-11}$
	4(4,0E)	9.2015768930	9.9351423485	8.6707439271	$\times10^{-9}$
	4(4,0F$_2$)	6.7123543060	7.1924201979	6.3637506536	$\times10^{-9}$
	5(1,0F$_1$)	-9.8901362804			$\times10^{-12}$
	5(3,0F$_1$)	-1.9792627703	-17.637866314	-10.458238360	$\times10^{-12}$
	5(5,0F$_1$)	4.7126915343	-14.685056098	-9.7397326174	$\times10^{-12}$
	5(5,1F$_1$)	-9.1292709636	-13.443072668	-11.009102070	$\times10^{-12}$
	6(0,0A$_1$)	-1.3207343178	-1.7812526042	0.8024915616	$\times10^{-13}$
	6(2,0E)	-1.4624471868			$\times10^{-13}$
	6(2,0F$_2$)	14.374793642	-2.2605424509	-2.2605424509	$\times10^{-14}$
	6(4,0A$_1$)	-8.2612218488	-4.8405037334	-4.8405037334	$\times10^{-15}$
	6(4,0E)	2.3983009358			$\times10^{-13}$
	6(4,0F$_2$)	1.7444078013			$\times10^{-13}$
$\nu_1+\nu_3$	0(0,0A$_1$)	-3.855453(66)	-3.94525(20)	-4.00663(17)	
	1(1,0F$_1$)	-2.9117(45)	-2.553(22)	-2.366(11)	$\times10^{-3}$
	2(0,0A$_1$)	-1.472(85)	-11.20(68)	-13.68(36)	$\times10^{-6}$
	2(2,0E)	3.368(42)	2.16(42)		$\times10^{-6}$
	2(2,0F$_2$)	-1.258(14)	-1.072(73)	-1.036(82)	$\times10^{-5}$
	3(1,0F$_1$)	-1.296(88)$\times10^{-8}$	1.25(17)$\times10^{-7}$	5.38(32)$\times10^{-8}$	
	3(3,0F$_1$)	1.646(69)	2.2(1.3)	1.59(43)	$\times10^{-8}$
	4(0,0A$_1$)	0.533(22)	5.69(50)	1.36(26)	$\times10^{-9}$
	d_{rms}	0.863	0.765	0.480	$\times10^{-3}$
	J_{max}	82	45	58	

* Values with no uncertainty are fixed to the fundamental band parameters [27].

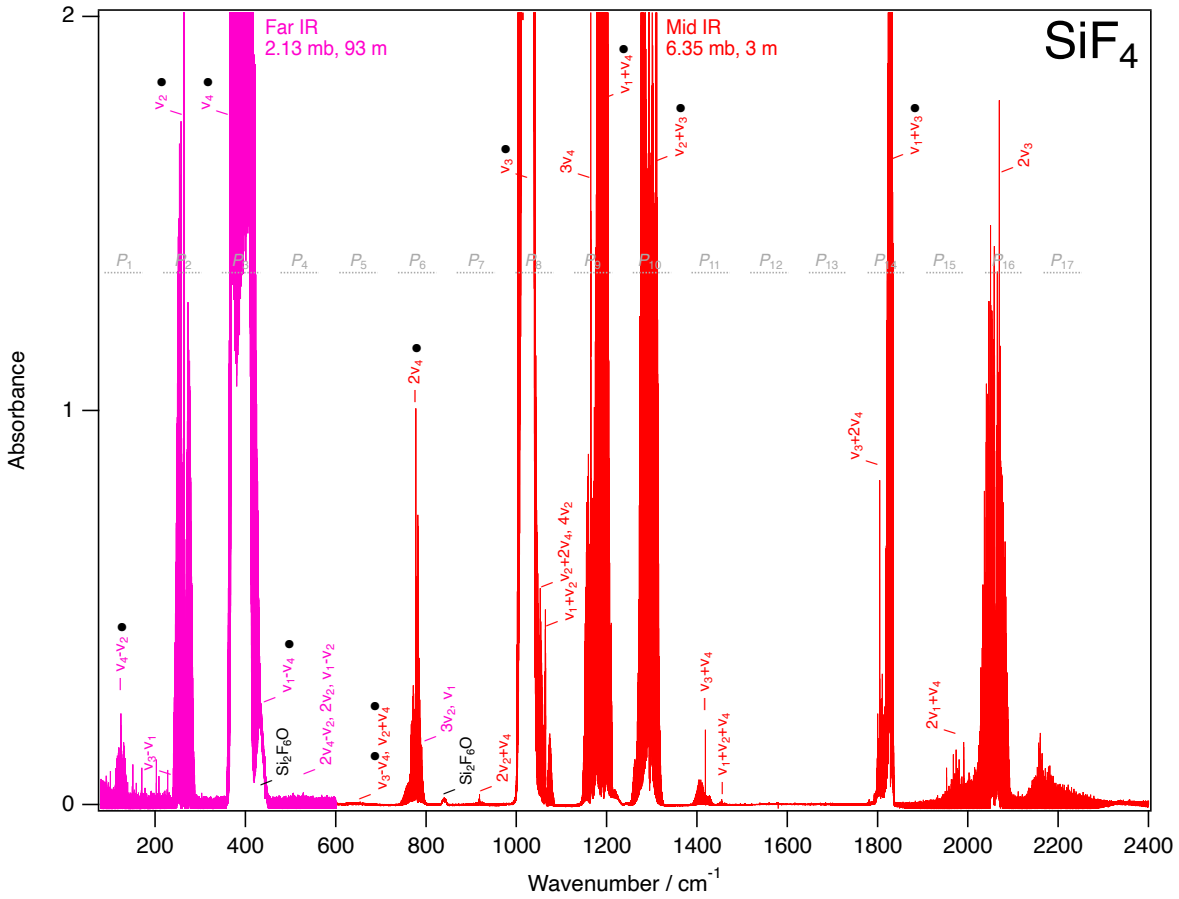

Figure 1: The global picture of the experimental spectra (pressure and path length are indicated at the top; for detailed experimental conditions, see section 2). The analyzed bands in [26, 27] and in the present work are marked by the black dots.

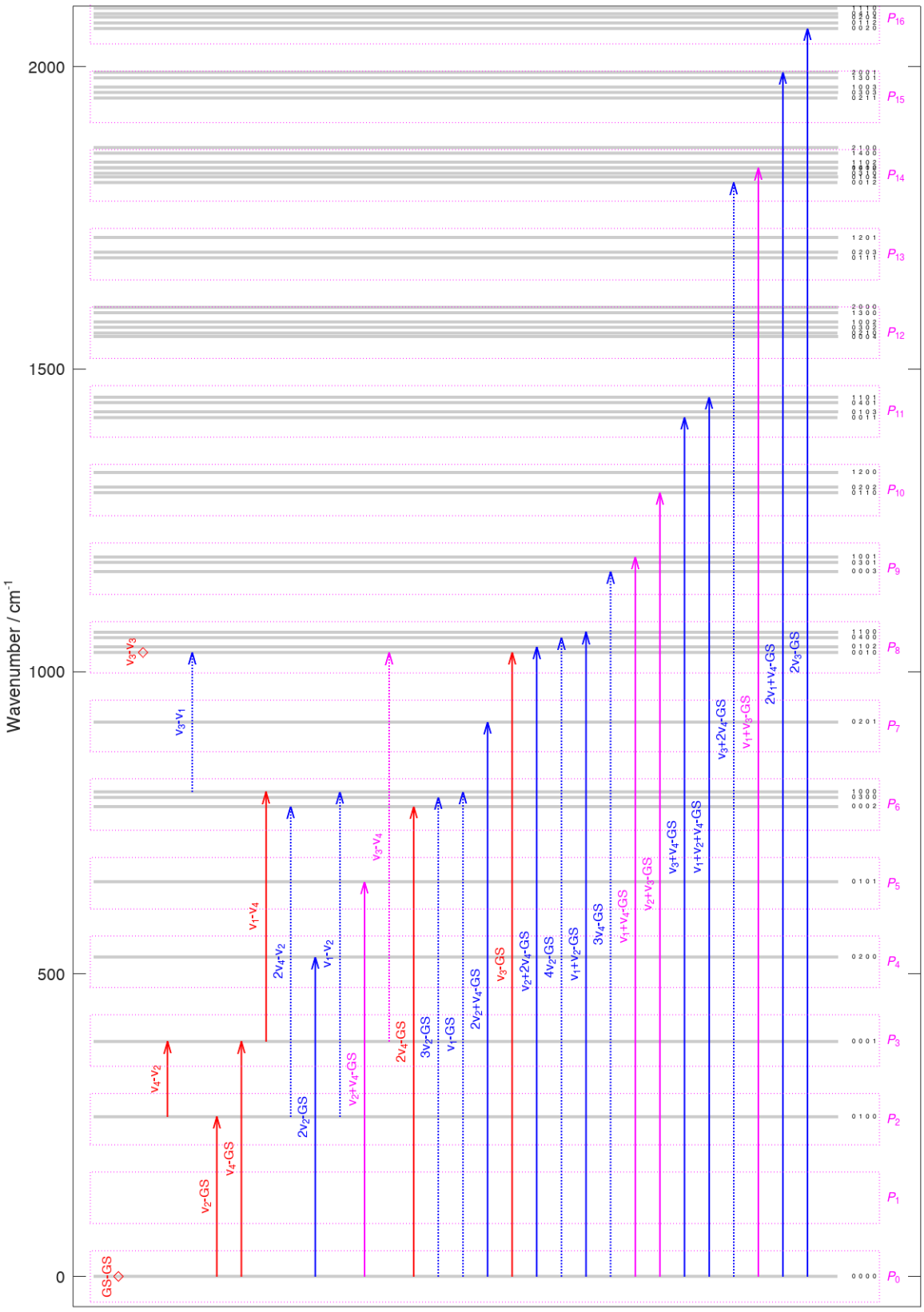

Figure 2: The vibrational levels of the SiF_4 molecule. The color markers are as follows given in the text.

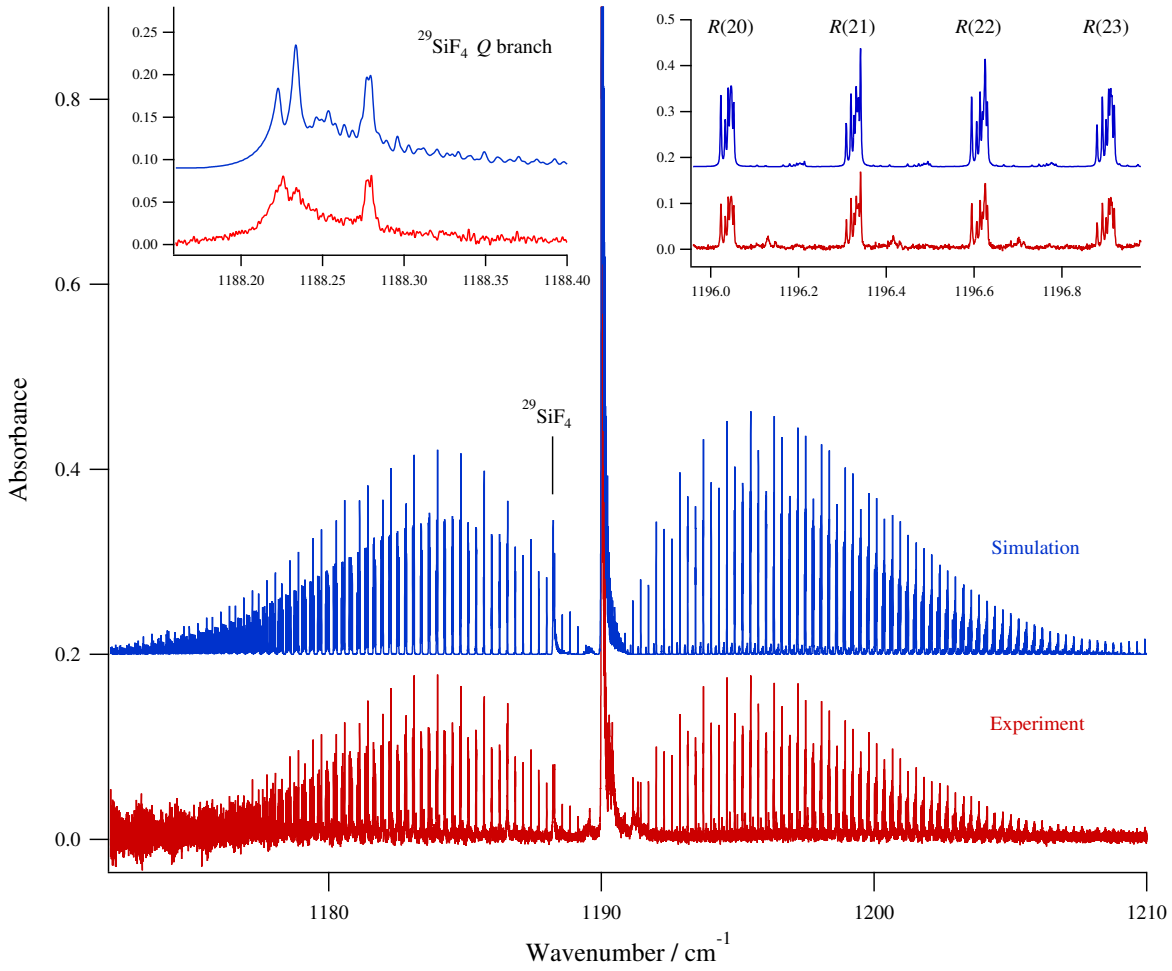

Figure 3: The $\nu_1+\nu_4$ band (see section 2 for experimental conditions), compared to the simulation. The inserts display a few line clusters in the R branch and zoomed image of the $^{29}SiF_4$ isotopologue band center.

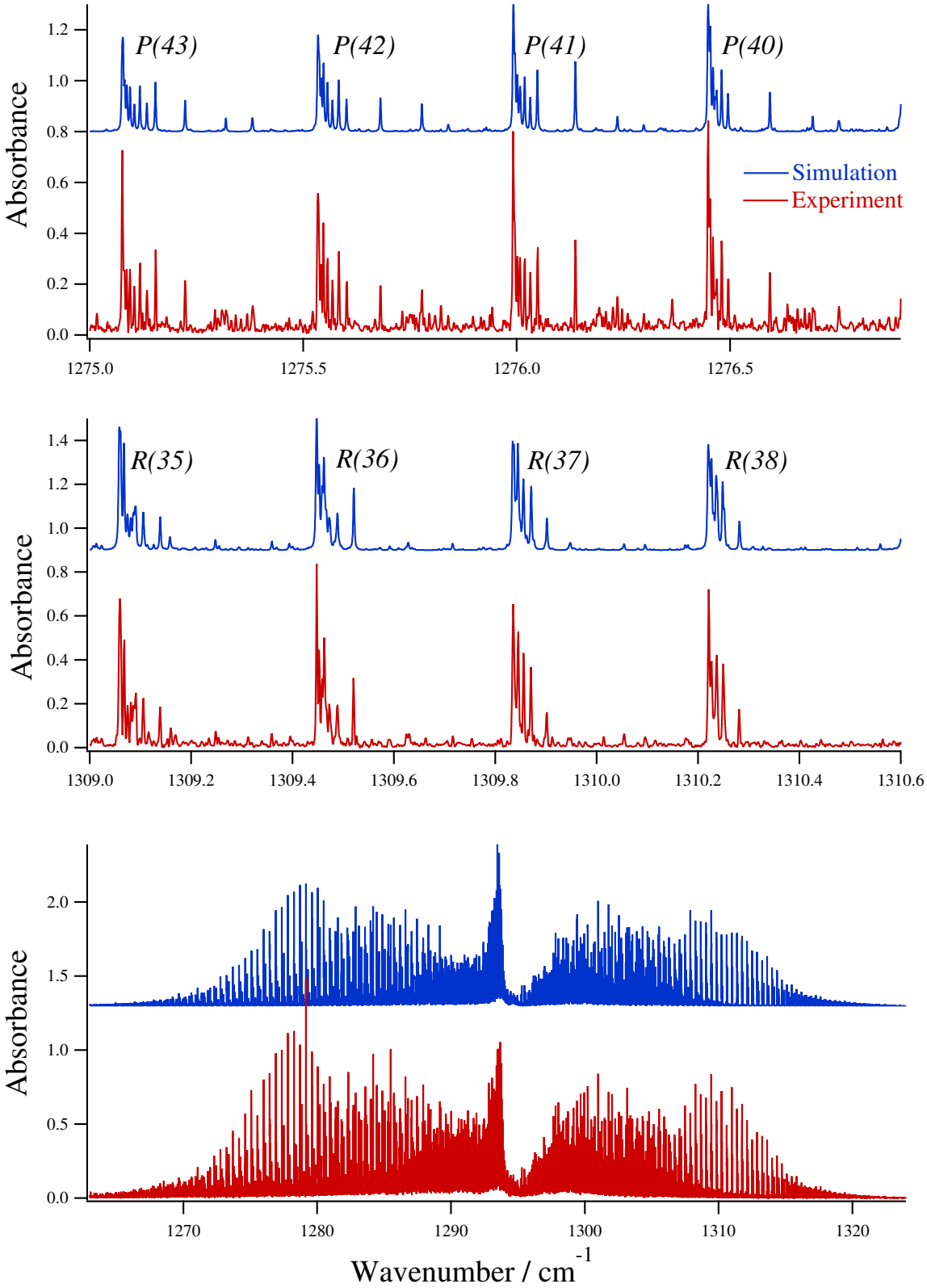

Figure 4: Comparison between the simulated and experimental (see section 2 for experimental conditions) spectra for the $\nu_2+\nu_3$ band: detail in P- and R-branch.

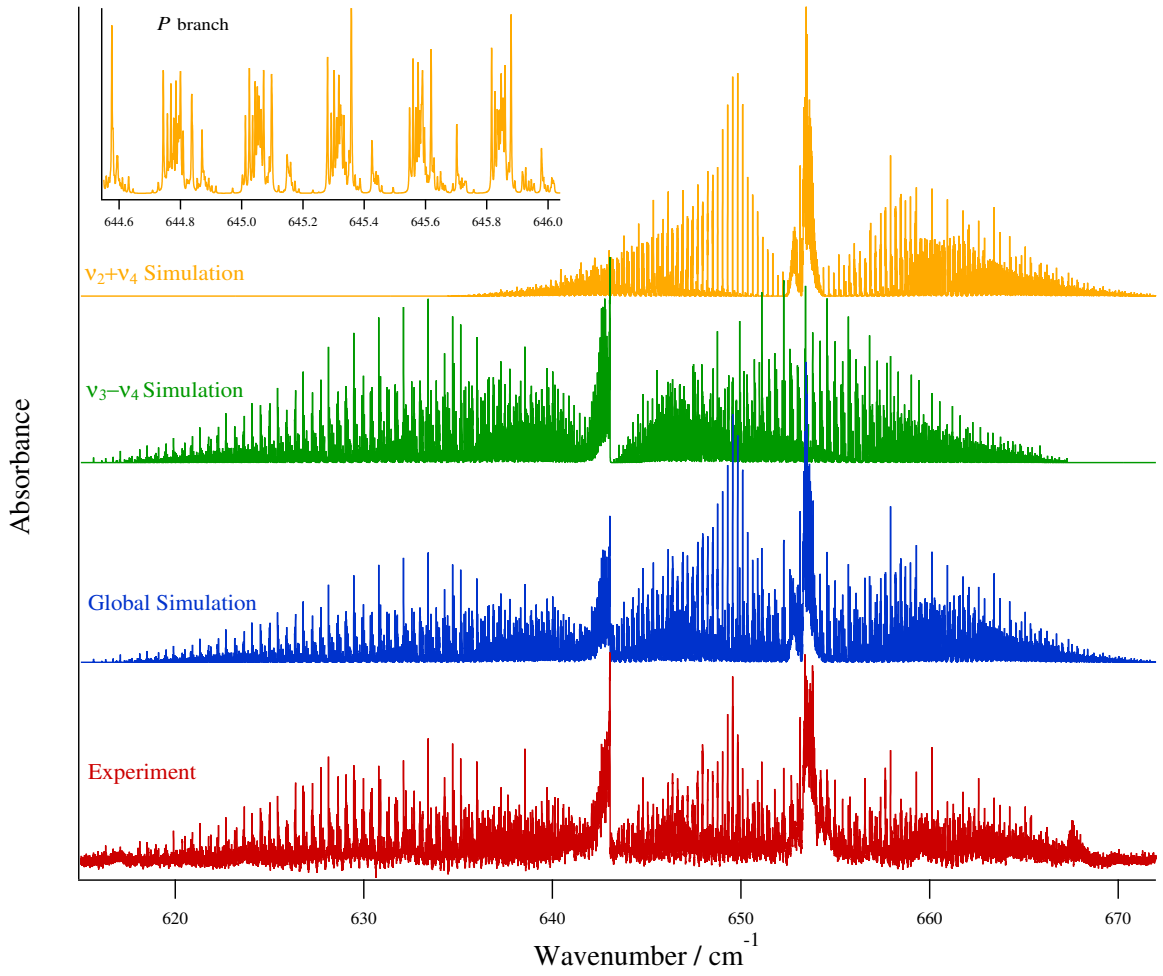

Figure 5: Overview of the ν_2+ν_4 and ν_3-ν_4 spectrum (see section 2 for experimental conditions), compared to the simulation. The insert details a part of the P branch region.

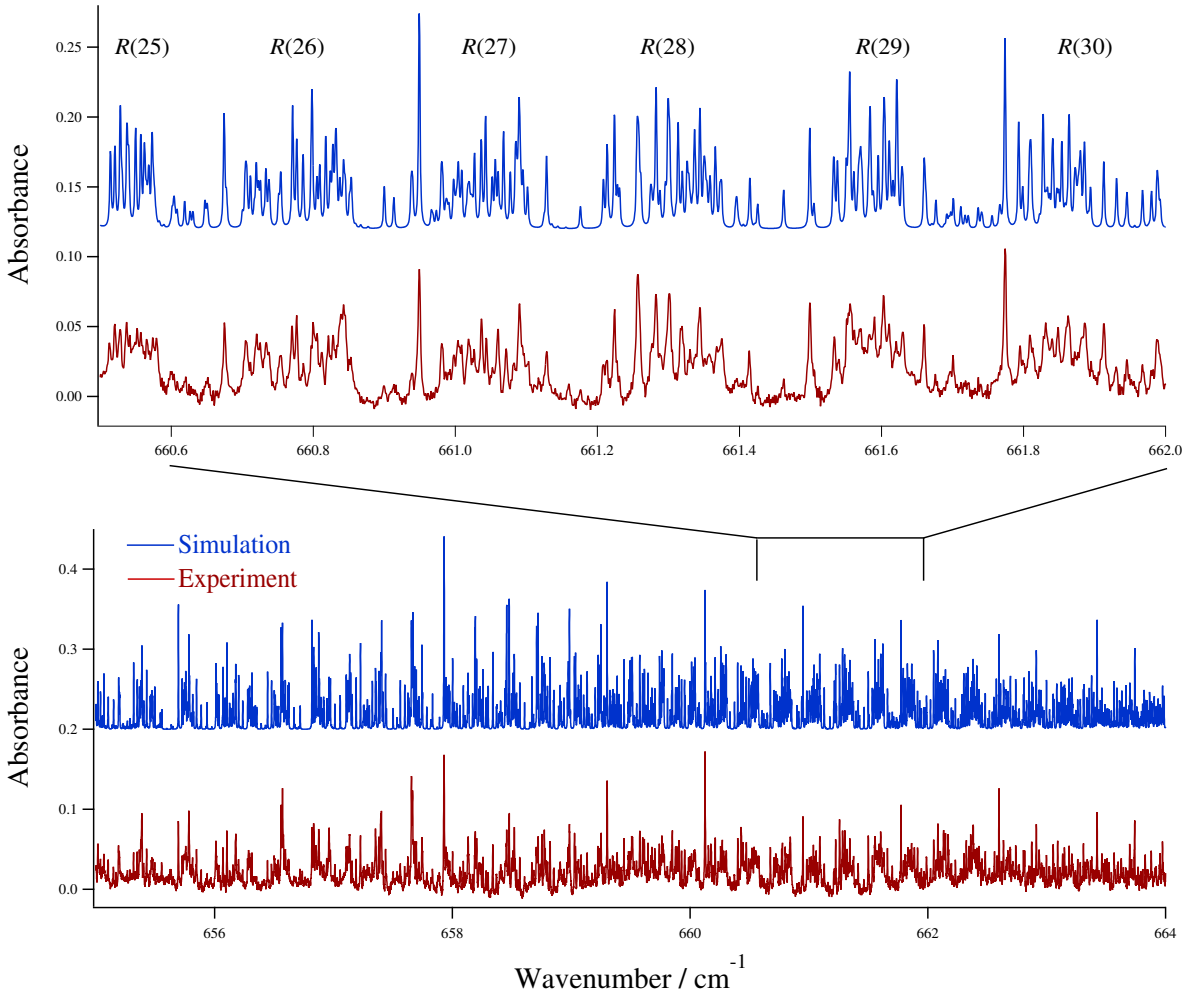

Figure 6: The $\nu_2+\nu_4$ spectrum: detail in R-branch.

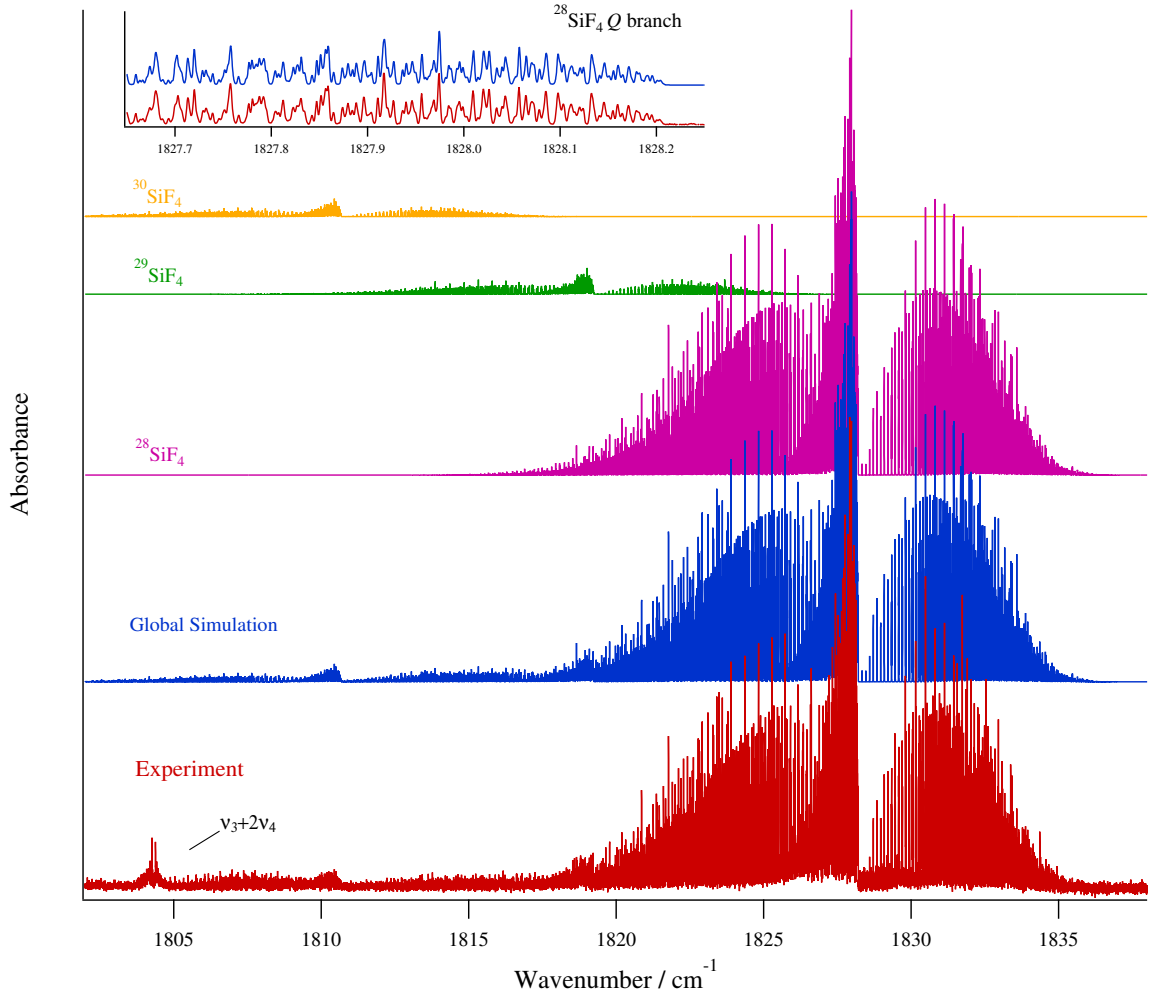

Figure 7: Overview of the $\nu_1+\nu_3$ spectrum (see section 2 for experimental conditions), compared to the simulation for all isotopologues. The insert details a part of the Q branch region.

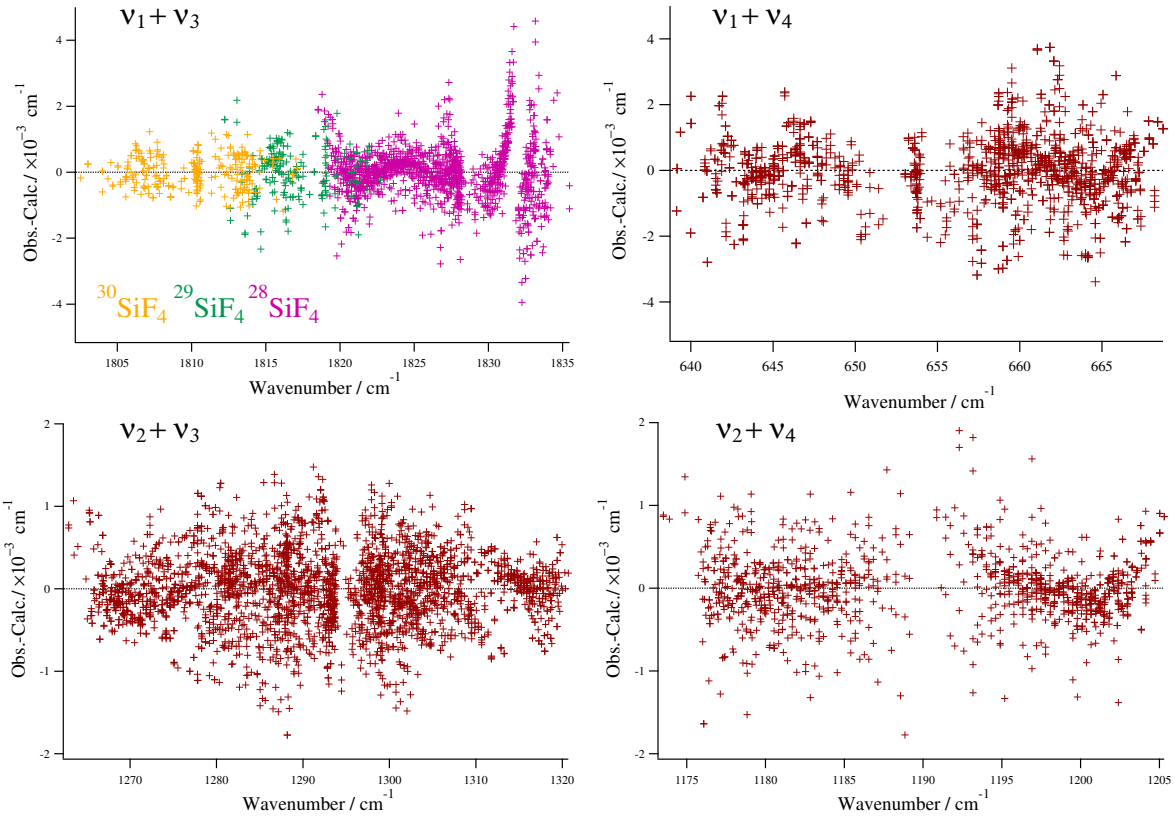

Figure 8: Fit residuals for line positions for each studied band.